RSC Advances

ROYAL SOCIETY OF CHEMISTRY

www.rsc.org/advances

Gold nanoparticles make chitosan-streptomycin conjugates effective to gram-negative bacterial biofilm

Haibo Mu[1], Qianjin Liu[1], Hong Niu, Yuelin Sun and Jinyou Duan*

College of science, Northwest A&F University, Yangling 712100, Shaanxi, China;

[1] These authors contributed equally to this work.

Correspondence:

Jinyou Duan, PhD;

Tel: +86 29-87082226; Fax: +86 29-87082226;

E-mail: jduan@nwsuaf.edu.cn

Abstract

The emergence of biofilm-associated resistance of microbe to traditional antibiotics has resulted in an urgent need for novel antimicrobial agents. Herein we developed a facile approach to overcome the problem through chitosan-streptomycin gold nanoparticles (CA NPs). The synthesized CA NPs were characterized by ultraviolet−visible absorption spectra (UV−vis), scanning electron microscopy (SEM), transmission electron microscopy (TEM) and dynamic light scattering (DLS). The resulted CA NPs maintained their antibiofilm activities to Gram-positive organisms. More importantly, CA NPs damaged established biofilms and inhibited biofilm formation of Gram-negative bacteria pathogens. Mechanistic insight demonstrated CA NPs rendered streptomycin more accessible into biofilms, thereby available to interact with biofilm bacteria. Additionally, CA NPs was observed to kill more biofilm-dispersed cells than CS conjugate or streptomycin and inhibit the planktonic cell growth of Gram-positive and -negative bacteria. Thus, this work represent an innovative strategy that gold nanoparticles linked to carbohydrate-antibiotic conjugation can overcome antibiotic resistance of microbial biofilms, suggesting the potential of using the generated CA NPs as antimicrobial agents for bacterial infectious diseases.

Keywords: gram-negative organism biofilm, chitosan, streptomycin, gold nanoparticle

1. Introduction

Microorganisms do not live as pure cultures of dispersed single cells but instead accumulate at interfaces to form highly structured multi-cell aggregates in a self-produced hydrated extracellular matrix as biofilms.[1] The formation of a biofilm are associated with many illnesses and infections in humans, including oral diseases, native valve endocarditis, and a number of nosocomial infections.[2]

Bacteria in biofilms which are heterogeneous microenvironments, featuring chemical gradients of important parameters such as oxygen, pH, and nutrients, display a different physiology compared to planktonic cells such as a diminished metabolic rate, and improved cell to cell communication, which makes antibiotics less effective and increases the chance of development of resistances.[3-5] Owing to the emergence and increasing prevalence of biofilm that are resistant to available antibiotics, new therapeutic approaches have been proposed include bacteriophage,[6] metal nanoparticles,[7-9] nanocarriers,[10, 11] synthetic small molecules,[12, 13] plant extracts[14] and chitosan derivatives,[15, 16] all of which have been shown to influence biofilm structures with different efficiencies via various mechanisms.

In our previous studies, we developed an innovative strategy to combat microbial biofilms by using chitosan as a covalent carrier for an aminoglycoside antibiotic, streptomycin.[17] The polycationic property enabled chitosan as an efficient Trojan horse to deliver streptomycin into biofilms, which made bacterial biofilms more susceptible to streptomycin at a lowest effective dose. Unfortunately, this was the case for biofilms built by all Gram-positive organisms tested, but not Gram-negative

organisms such as *P. aeruginosa* and *S. typhimurium*. One main factor is the inability of the antibiotic to penetrate into Gram-negative bacterial biofilms.

Gold nanoparticles (Au NPs) have been extensively used in drug delivery applications, intracellular gene regulation, bioimaging, anti-inflammatory therapy and anticancer therapy, due to their attractive optical and electronic properties, easy surface functionalization and excellent biocompatibility.[18, 19] Furthermore, the antimicrobial activity of gold nanoparticles has been recently demonstrated which strongly depends on the size, shape and surface modifications of Au NPs, although their mechanism of bacterial growth inhibition remains still unclear.[20-22]

Gold nanoparticle (Au NPs) have been coupled with known antibiotics via covalent bonds to enhance activity against bacteria, showing decreased minimum inhibitory concentration (MIC) in comparison with use of free antibiotics.[23, 24] The improved performance is proposed to result from polyvalent effect of concentrated antibiotics on the NP surface as well as enhanced internalization of antibiotics by Au NPs.[25] To this end, we set out to upgrade the chitosan-streptomycin conjugates (CS) by introducing Au NPs. Herein, we synthesized CA NPs using CS as capping agent and investigated their antibiofilm properties against Gram-negative and Gram-positive organisms. And also their antimicrobial properties against planktonic bacteria were determined.

2. Experimental methods

2.1. Materials

Streptomycin Sulfate was purchased from Solarbio (Beijing, China).

Phosphatidylcholine and Hydrogen tetrachloroaurate ($HAuCl_4$), sodium borohydride ($NaBH_4$) and Sodium cyanoborohydride ($NaBH_3CN$) were purchased from Aladdin (Shanghai, China). Chitosan (13KDa, 88%DD) was purchased from Qingdao Yunzhou Bioengineering Co. Ltd. (Qingdao, China). Sodium nitroprusside (SNP) was was obtained from Beyotime Institute of Biotechnology (Shanghai, China). All reagents were of analytical grade and used as received without further purifying.

2.2. Bacterial strains and growth conditions

Listeria monocytogenes (ATCC 19114), *Staphylococcus aureus* (ATCC 29213), *Escherichia coli* (ATCC 25922), *Pseudomonas aeruginosa* (PAO1) and *Salmonella typhimurium* (SL1344) were generous gifts received from Prof. Xia (College of Food Science and Engineering, Northwest A&F University). The strains were cultured in Tryptone Soya broth (TSB) at 37 °C, and the grown culture was used for inoculation into the wells of plastic microtiter plate (Corning, NY) for subsequent quantification of biofilm production.

2.3. Preparation of CA NPs

Chitosan-streptomycin conjugates (CS) were prepared following a previously described method.[17] Briefly, 2.712 g of streptomycin sulfate and 50 mg of chitosan were dissolved in 20 mL deionized water, followed by addition of 0.372 g $NaCNBH_4$. The reaction mixture was stirred for 15 h in the dark and then dialyzed 2 days and finally lyophilized. Streptomycin contents in conjugates were determined through quantification of guanidyl groups and streptomycin sulfate was used as a standard.[26]

CA-1 were prepared by a sodium borohydride reduction method.[27] Briefly, 16 mL

aqueous solution of $HAuCl_4$ (0.4 mM) was reduced by 0.1 mL ice-cold $NaBH_4$ (16 mg/mL) to prepare bare gold nanoparticles. The acquired bare gold nanoparticles solution was then mixed overnight with CS (2mg/mL, 16 mL) that was predissolved in deionized water. The resulting solution initially centrifuged at 14 000 rpm at 10 °C for 40 min and the AuCS-1was rinsed in ultra-pure H_2O.

CA-2 were conducted by chemical reduction of $HAuCl_4$/CS mixtures with sodium borohydride.[28] For a typical experiment, 16 μL of freshly prepared $HAuCl_4$ (200 mM) was added to 8 mL of CS (1 mg/mL), and the solutions were stirred for 1 h. Then, 40 μL of freshly prepared ice-cold $NaBH_4$ (0.4 M) was quickly added to the solutions under stirring and left stirring for 30 min.

UV-vis absorbance spectrum of CA NPs from 300 to 600 nm was recorded by a spectrophotometer (Thermo Evolution 300). The morphology of the CA NPs was characterized by Hitachi S-4800 field emission scanning electron microscopy (SEM) and Hitachi H-7700 transmission electron microscopy (TEM) (Hitachi, Japan), operating at an accelerating voltage of 10 kV and 80 kV respectively. The hydrodynamic size and surface zeta potential of the prepared CA NPs were measured by dynamic light scattering (DLS) measurements (Malvern Zetasizer NANO-ZS90, Malvern, UK).

2.4. Antibiofilm Activity

As described previously,[29] 100 μL bacterial TSB solutions (~10^8 cfu) were seeded into 96-well polystyrene microtitre plates (Corning, NY, USA) at 37 °C for 24 h to allow biofilm formation. The non-adhered cells were removed with pipette and the plate was washed three times using 100 μL 0.9% (w/v) NaCl. Then existing biofilms

were incubated at 37 °C in TSB supplemented with compounds for 24 h. Each treatment included 6 parallel wells. Biofilms incubated in TSB containing PBS were used as blank control. Biofilm was evaluated by serial dilution plate counting method. All experiments were performed 3-5 times. Error bars represent SD.

For biofilm inhibition assay, one hundred microlitres of bacteria in TSB (approximately 10^8 cfu) were seeded into individual wells of microtiter plates in the presence of compounds for 24 h. Biofilm were evaluated as described above.

For fluorescence microscopy, *S. aureus or P. aeruginosa* (~10^8 cfu) was grown on glass coverslips at 37 °C for 24 h in 24-well plates supplemented with 1 mL of TSB to allow biofilm formation. The coverslips were washed to remove unattached cells and were treated with CA NPs or equivalent streptomycin for 24 h at 37 °C. Existing biofilms were treated and imaged as previous.[29]

SEM was conducted as described previously.[30]

2.5. Immunofluorescence

As mentioned in fluorescence microscopy assay, biofilms on glass coverslips were fixed in 4% paraformaldehyde. After treatment with 0.25% Triton X-100 and blocking with 1% BSA in PBS, coverslips were incubated with a polyclonal antibody for streptomycin (rabbit anti-gentamicin ployclone, Abcam, Cambridge, MA, USA) at 4 °C overnight, and then incubated with a second Dylight 405-goat anti-rabbit IgG for fluorescence microscopy (Jackson Immuno Research Inc., West Grove, PA, USA). Immunoreactivity was quantified by using Image Pro Plus (Media Cybernetics, Silver Spring, MD, USA).

2.6. Biofilm-dispersed cells

To generate dispersed cells, the preformed biofilms (72 h) were washed three times with 0.9% NaCl and resuspended in TSB containing 5 mM SNP for 3 h at 37 °C. Then the cells were incubated in the presence of compounds for 24 h. Then 10 μL samples was collected and incubated in 190 μL TSB for 14 h and the optical density at a wavelength of 600 nm (OD_{600}) was record.

2.7. Antibacterial activity

Bacteria samples (0.4 OD_{600}, 0.5 mL) were mixed well with TSB (19.5 mL) including different concentrations of CA NPs. The mixtures were shaken at 37 °C. The OD_{600} was monitored at intervals.

2.8. Cytotoxicity Tests

The RAW 264.7 cell line was cultured in RPMI medium supplemented with 10% FBS, 100 μg/mL penicillin and 100 μg/mL streptomycin at 37 °C in a humidified 5% CO_2-contaning balanced-air incubator.

Cytotoxicity of CA NPs was evaluated by MTT assay. The 200 μL cells (~8000 cells) were incubated for 12 h in 96-well plates, then the medium was replaced with the medium containing different concentrations of CA NP and incubated for another 12 h. After treatment, cell viability were estimated as previous.[31]

2.8. Statistical analysis

All graphical evaluations were made using GraphPad Prism 5.0 (GraphPad Software Inc., San Diego, CA). The data are expressed as means ± SD with the statistical method of One-way ANOVA followed by unpaired t-test. $p < 0.05$ was considered statistical significance.

3. Results and Discussions

3.1. Synthesis and Characterization of CA NPs

CA NPs in this work were synthesized by chemical reduction of $HAuCl_4$ (denoted as CA-1) or $HAuCl_4$/CS mixtures (denoted as CA-2) with sodium borohydride. The equal amounts of $HAuCl_4$ and CS were used in both two methods. It is well known that gold nanoparticles exhibit a ruby red color in aqueous solution due to the surface plasmon resonance (SPR) of metal nanoparticles.[24] The generated product solution was red in color indicating the formation of gold nanoparticles. As shown in Fig. 1A, the absorption spectrum of CA-1 and CA-2 had a maximum absorption band at 531nm and 545nm, respectively. Dynamic light scattering (DLS) measurements showed that the size of CA-1 and CA-2 were 31 nm and 45 nm (Fig. 1B) with positive surface ζ potential of 18.7 mV and 25.0 mV respectively (Fig. 1C). The morphology of the CA NPs was imaged by SEM (Fig. 1D) and TEM (Fig. 1E).

3.2. CA NPs disrupted preformed biofilms of Gram-negative and Gram-positive microorganism

P. aeruginosa is a Gram-negative opportunistic human pathogen, which is generally employed as a model organism for investigation of biofilms.[32] Streptomycin alone had a mild effect on biomass of *P. aeruginosa* biofilms after 24 h treatment compared to blank control (Fig. 2A). CA NPs improved the reduction of biofilm dramatically compared to CS conjugate or streptomycin treatment, although CS conjugate, Au NPs (bare gold nanoparticles) or chitosan-Au NPs treatment didn't reduce biofilm at all (Fig. S1). Concentration-dependent analysis further confirmed that CA NPs at various concentrations (125, 250, 500 μg/mL) was more efficient in

disruption of *P. aeruginosa* biofilms than CS conjugate or streptomycin (Fig. S2). In addition, viability tests indicated that the cytotoxicity of the GPA NPs towards macrophages was negligible below 400 μg/mL (Fig. S3). For *S. typhimurium*, another Gram-negative bacterium which is a rod-shaped foodborne pathogens,[33] a similar findings were also observed (Fig. 2B). These results indicated that CA NPs were able to disperse the existing biofilms built by Gram-negative organisms. To see whether CA NPs still possessed the ability of CS conjugate to smash up bacterial biofilms built by Gram-positive organisms, *L. monocytogenes* (Fig. 2C) and *S. aureus* (Fig. 2D), both of which can cause life-threatening infections in humans and the nosocomial (hospital) environment,[34, 35] were tested. Quantification of biofilm cell demonstrated that CA-1 NPs had a more pronounced effect than CS conjugate or streptomycin alone did, although CA-2 NPs didn't further reduce biofilm compared to CS conjugate ($p > 0.05$). Overall, these results clearly indicated that CA NPs had an ability to disrupt existing biofilms formed by Gram-negative and -positive organisms

Fluorescence microscopy imaging of *P. aeruginosa* (rod-shaped pathogen, Fig. 2E) and *S. aureus* (round-shaped pathogen, Fig. 2F) biofilms was pursued to further evaluate the antibiofilm potential of CA NPs. The blank control biofilms were densely colonized with hierarchically and three-dimensionally structured formations as shown in Fig. 2E. No significant changes were observed in the biofilms treated with CS conjugate compared to blank biofilms. In contrast, biofilms treated with streptomycin showed a moderate reduction of total biofilm with a scanty architecture. Most significantly, the biofilm treated with CA NPs exhibited only a few isolated bacterial

colonies instead of a recognizable biofilm structure. Thus, these qualitative findings further confirmed that the newly synthesized CA NPs possessed superior antibiofilm properties over free-form streptomycin.

SEM microscopy was applied to evaluate the surface morphology changes of treated *P. aeruginosa* (Fig. 2G) and *S. aureus* (Fig. 2E) with CA NPs in TSB. As shown in Fig. 2G, both control and CS treated biofilms exhibited dense colonization with a clearly visible extracellular matrix. These biofilms showed highly organized and well-defined architecture. Streptomycin-treated biofilms demonstrated general disruption of the biofilm structure and showed some evidence of organization throughout the remaining bacterial cells with some quantities of aggregates visible. However in CA NPs-treated biofilms, the cell walls of *P. aeruginosa* became wrinkled and damaged with its shape and size of cells changed dramatically, and only a few scattered bacterial cells were noted. The similar phenomena also can be seen in *S. aureus* biofilms, although CS had good efficacy in destroying biofilms built by Gram-positive organism (Fig. 2H). These results confirmed that CA NPs could severely disrupt the biofilm architecture and destroyed biofilm cells structure of both Gram-negative and -positive bacteria.

3.3. CA NPs prevent bacterial biofilm formation

Biofilm formation was examined in case of planktonic *P. aeruginosa* (Fig. 3A) exposed to compounds for 24 h at the beginning. CS conjugate showed no effects on biofilm formation as compared with blank control. The free-form streptomycin suppressed biofilm formation a little whereas CA NPs facilitated this suppression

significantly. Likewise, the CA NPs were more effective against *S. typhimurium* biofilm than CS conjugate or streptomycin alone (Fig. 3B). The similar findings were also observed in case of *L. monocytogenes* (Fig. 3C) and *S. aureus* (Fig. 3D) by quantification of biofilm CFU. Visualization of *P. aeruginosa* biofilms (Fig. 3E) and *S. aureus* (Fig. 3F) with scanning electron microscopy, showed a wide spectrum of morphological differences in cell morphology and biofilm architecture. Notably, fewer scattered cell aggregates were observed in the biofilms after 24 h exposure to CA NPs and there were more broken cells in the aggregates.

Collectively, the aforementioned results suggested that CA NPs had a potential to prevent planktonic cells of Gram-negative or -positive organisms from biofilm formation.

3.4. CA NPs inhibited biofilm-dispersed cells replication

Biofilm development requires specific steps and is typically described as a four-step process: initial contact, attachment, maturation, and dispersion.[36] The cells from programmed biofilm dispersal belong to an important and unique intermediate phase in the biphasic life cycle of bacteria. The biofilm-dispersed cells show different styles and highly virulent compared to planktonic cells.[37] To explore efficacy of CA NPs against biofilm-dispersed cells, preformed biofilm were washed three times with 0.9% NaCl and treated with SNP for 3 h to allowed bioflim dispersion, and then incubated for 16 h with CA NPs or streptomycin. As shown in Fig. 4A, optical density at 600nm measurements suggested that both two nanoparticles were more effective in prevention of *P. aeruginosa* biofilm-dispersed cells replication, compared to CS conjugate or free-form streptomycin. Also, CA NPs were more effective against

another Gram-negative organism *S. typhimurium* biofilm-dispersed cells (Fig. 4B). Again, the similar findings were observed in case of *L. monocytogenes* (Fig. 4C) and *S. aureus* (Fig. 4D).

3.5. CA NPs exhibited obvious effect of growth inhibition on planktonic bacteria

These aforementioned observations raised the question whether CA NPs had a priority in killings of planktonic organisms when compared with CS conjugate or streptomycin alone, despite the fact that CS conjugate exhibited a similar bactericidal ability to streptomycin.[17] The bactericidal activity of CA NPs and streptomycin were tested to *S. typhimurium* and *S. aureus* on different concentrations (Fig. S4). Fig. 5A shows the growth curves of *S. typhimurium* obtained by culturing bacteria in TSB containing CA NPs, equivalent CS conjugate or streptomycin. The results show that the cell growth of *S. typhimurium* was effectively inhibited by CA NPs (250 μg/mL) compared with the blank curve obtained from culturing *S. typhimurium* in TSB. By contrast, less effective inhibition of the bacterial cell growth was observed when the bacterial samples were treated with CS conjugate or free-form streptomycin. Meanwhile, the CFU was counted at 8 h time point by culturing the 100 μL samples (10^7 dilution) on Petri dishes. Fig. 5B shows the overnight culture results of *S. typhimurium* cells mixed with and CA NPs respectively. Apparently, many bacterial colonies were observed with CS conjugate or streptomycin treatment. However, no colonies were observed in treatment with CA NPs. As expected, CA NPs also showed strong inhibition in *S. aureus* grown compared to streptomycin (Fig. 5C and D). These results indicated that CA had a superior ability to suppress planktonic cells growth.

3.6. Mechanistic insights into the anti-biofilm capability of CA NPs

CS conjugates was ineffective to remove biofilms built by Gram-negative organisms.[17] One important factor is that the biofilm matrix might act as an adsorbent or reactant, thereby reducing the amount of agent available to interact with biofilm cells.[38] Given gold nanoparticle possesses fine penetration and has been used as a carrier of antibiotics for selective killing of diseased microbes,[39-41] we attempted to see whether CA NPs facilitated streptomycin entry into biofilms. Using a polyclonal antibody to streptomycin produced in rabbit and a second Dylight 405-conjugated goat anti-rabbit IgG, streptomycin residing in established biofilms was visualized. *P. aeruginosa* biofilms exposed to CS conjugate or streptomycin alone exhibited a weak blue fluorescence (Fig. 6A). In contrast, the intense blue fluorescence was observed after treated with CA NPs, which suggested that CA NPs made more streptomycin access into biofilms built by *P. aeruginosa*. Similarly, more brilliant blue fluorescence was detected in *L. monocytogenes* biofilms exposed to CA NPs (Fig. 6B).

4. Conclusion

Bacterial biofilms are responsible for several chronic diseases that are difficult to treat. One potential reason for this increased resistance is the penetration barrier that biofilms may present to traditional antibiotics. We overcome this successfully by conjugating chitosan to streptomycin to increase the ability of antibiotic against biofilms built by Gram-positive organisms, but not Gram-negative bacteria.

In this study, we developed a robust nanoparticle by introducing gold nanoparticles (Au) to chitosan-streptomycin conjugate (CS), named CA NPs. Excitingly, such nanoparticle had violent biofilm disruption activity on Gram-negative

bacteria. Also, these CA NPs retained the ability to eradicate formed biofilm and inhibit the biofilm formation of Gram-positive bacteria. Moreover, CA NPs displayed favorable bactericidal effects on both Gram-negative and -positive organisms when compared with the same concentrations of CS conjugate or free streptomycin. These results indicated the potential of the generated CA NPs can be used as powerful antibacterial agents to biofilm. Our results indicate that the use of gold nanoparticles to upgrade chitosan-streptomycin conjugates represents a promising strategy for developing effective antibacterial regimes.

Acknowledgments

This work was supported by the National Natural Science Foundation of China (NSFC31570799).

References

1. L. Hall-Stoodley, J. W. Costerton and P. Stoodley, *Nat Rev Micro*, 2004, **2**, 95-108.
2. P. Stoodley, K. Sauer, D. G. Davies and J. W. Costerton, *Annual Review of Microbiology*, 2002, **56**, 187-209.
3. H.-C. Flemming and J. Wingender, *Nature Reviews Microbiology*, 2010, **8**, 623-633.
4. E. Drenkard and F. M. Ausubel, *Nature*, 2002, **416**, 740-743.
5. P. S. Stewart and M. J. Franklin, *Nat Rev Micro*, 2008, **6**, 199-210.
6. T. K. Lu and J. J. Collins, *Proceedings of the National Academy of Sciences*, 2007, **104**, 11197-11202.
7. R. P. Allaker, *Journal of Dental Research*, 2010, **89**, 1175-1186.
8. L. Mei, Z. Lu, X. Zhang, C. Li and Y. Jia, *ACS Appl Mater Interfaces*, 2014, **6**, 15813-15821.
9. R. Pati, R. K. Mehta, S. Mohanty, A. Padhi, M. Sengupta, B. Vaseeharan, C. Goswami and A. Sonawane, *Nanomedicine*, 2014, **10**, 1195-1208.
10. A. Baelo, R. Levato, E. Julian, A. Crespo, J. Astola, J. Gavalda, E. Engel, M. A. Mateos-Timoneda and E. Torrents, *J Control Release*, 2015, **209**, 150-158.
11. K. Forier, A. S. Messiaen, K. Raemdonck, H. Nelis, S. De Smedt, J. Demeester, T. Coenye and K. Braeckmans, *J Control Release*, 2014, **195**, 21-28.
12. J. Hoque, M. M. Konai, S. Samaddar, S. Gonuguntala, G. B. Manjunath, C. Ghosh and J. Haldar, *Chemical Communications*, 2015, **51**, 13670-13673.
13. R. Frei, A. S. Breitbach and H. E. Blackwell, *Angewandte Chemie International Edition*, 2012, **51**, 5226-5229.

14. A. Adonizio, K.-F. Kong and K. Mathee, *Antimicrobial Agents and Chemotherapy*, 2008, **52**, 198-203.
15. B. Orgaz, M. M. Lobete, C. H. Puga and C. San Jose, *International Journal of Molecular Sciences*, 2011, **12**, 817-828.
16. L. R. Martinez, M. R. Mihu, G. Han, S. Frases, R. J. B. Cordero, A. Casadevall, A. J. Friedman, J. M. Friedman and J. D. Nosanchuk, *Biomaterials*, 2010, **31**, 669-679.
17. A. Zhang, H. Mu, W. Zhang, G. Cui, J. Zhu and J. Duan, *Sci. Rep.*, 2013, **3**, 3364.
18. E. Boisselier and D. Astruc, *Chemical Society Reviews*, 2009, **38**, 1759-1782.
19. P. Ghosh, G. Han, M. De, C. K. Kim and V. M. Rotello, *Advanced Drug Delivery Reviews*, 2008, **60**, 1307-1315.
20. S. K. Boda, J. Broda, F. Schiefer, J. Weber-Heynemann, M. Hoss, U. Simon, B. Basu and W. Jahnen-Dechent, *Small*, 2015, **11**, 3183-3193.
21. Y. Zhou, Y. Kong, S. Kundu, J. D. Cirillo and H. Liang, *J Nanobiotechnology*, 2012, **10**, 19.
22. A. Regiel-Futyra, M. Kus-Liskiewicz, V. Sebastian, S. Irusta, M. Arruebo, G. Stochel and A. Kyziol, *ACS Appl Mater Interfaces*, 2015, **7**, 1087-1099.
23. H. Z. Lai, W. Y. Chen, C. Y. Wu and Y. C. Chen, *ACS Appl Mater Interfaces*, 2015, **7**, 2046-2054.
24. A. Rai, A. Prabhune and C. C. Perry, *Journal of Materials Chemistry*, 2010, **20**, 6789-6798.
25. X. Li, S. M. Robinson, A. Gupta, K. Saha, Z. Jiang, D. F. Moyano, A. Sahar, M. A. Riley and V. M. Rotello, *ACS Nano*, 2014, **8**, 10682-10686.
26. P. D.C., V. S. J.F. and B. A.D.P., *Water S A*, 1991, **17**, 273-280.
27. D. Pornpattananangkul, L. Zhang, S. Olson, S. Aryal, M. Obonyo, K. Vecchio, C.-M. Huang and L. Zhang, *Journal of the American Chemical Society*, 2011, **133**, 4132-4139.
28. X. Zhou, X. Zhang, X. Yu, X. Zha, Q. Fu, B. Liu, X. Wang, Y. Chen, Y. Chen, Y. Shan, Y. Jin, Y. Wu, J. Liu, W. Kong and J. Shen, *Biomaterials*, 2008, **29**, 111-117.
29. H. Mu, A. Zhang, L. Zhang, H. Niu and J. Duan, *Food Control*, 2014, **38**, 215-220.
30. H. Mu, F. Guo, H. Niu, Q. Liu, S. Wang and J. Duan, *International Journal of Molecular Sciences*, 2014, **15**, 22296-22308.
31. H. Mu, A. Zhang, W. Zhang, G. Cui, S. Wang and J. Duan, *International Journal of Molecular Sciences*, 2012, **13**, 9194-9206.
32. L. Ma, M. Conover, H. Lu, M. R. Parsek, K. Bayles and D. J. Wozniak, *PLoS Pathogens*, 2009, **5**, e1000354.
33. M. K. Stewart, L. A. Cummings, M. L. Johnson, A. B. Berezow and B. T. Cookson, *Proceedings of the National Academy of Sciences*, 2011, **108**, 20742-20747.
34. V. Ferreira, M. Wiedmann, P. Teixeira and M. J. Stasiewicz, *Journal of Food Protection*, 2014, **77**, 150-170.
35. S. F. FitzGerald, J. O'Gorman, M. M. Morris-Downes, R. K. Crowley, S. Donlon, R. Bajwa, E. G. Smyth, F. Fitzpatrick, P. J. Conlon and H. Humphreys, *Journal of Hospital Infection*, 2011, **79**, 218-221.
36. P. Vogeleer, Y. D. N. Tremblay, A. A. Mafu, M. Jacques and J. Harel, *Frontiers in Microbiology*, 2014, **5**, 317.
37. S. L. Chua, Y. Liu, J. K. Yam, Y. Chen, R. M. Vejborg, B. G. Tan, S. Kjelleberg, T. Tolker-Nielsen, M. Givskov and L. Yang, *Nat Commun*, 2014, **5**, 4462.
38. D. Davies, *Nat Rev Drug Discov*, 2003, **2**, 114-122.
39. S. Khan, F. Alam, A. Azam and A. U. Khan, *Int J Nanomedicine*, 2012, **7**, 3245-3257.

40. G. Han, P. Ghosh and V. M. Rotello, *Nanomedicine*, 2007, **2**, 113-123.
41. Y. Zhao and X. Jiang, *Nanoscale*, 2013, **5**, 8340-8350.

Figure legend:

Fig. 1 Characterization of CA NPs. (A) Absorption spectrum of CA-1 and CA-2; Hydrodynamic size (B) and Surface zeta potential (C) of Bare Au NPs, CA-1 and CA-2 measured by dynamic light scattering; (D) SEM images and (E) TEM images of CA-1 and CA-2, scale bar represented 100 nm.

Fig. 2 CA NPs were effective against preformed biofilms built by Gram-negative and Gram-positive organisms. Biofilms formed by *P. aeruginosa* (A), *S. typhimurium* (B), *L. monocytogenes* (C) or *S. aureus* (D) were exposed to 250 μg/mL CA NPs, 250 μg/mL CS or equivalent 50 μg/mL streptomycin (Strep) for 24 h. Biofilms incubated in TSB containing PBS were used as blank control. Biofilm cells were quantified by serial dilution plate counting method. Preformed biofilm architectures after 24 h treatment were further examined by fluorescence microscopy (E: *P. aeruginosa*; F: *S. aureus*) and scanning electron microscopy (G: *P. aeruginosa*; H: *S. aureus*). These experiments were performed three times with similar results each time. Error bars represent standard deviation. Scale bar for fluorescence microscopy represented 10 μm, Scale bar for scanning electron microscopy represented 400 nm.

Fig. 3 CA NPs inhibited bacterial biofilm formation. The following bacteria were seeded in 96-well plates in the presence of 250 μg/mL CA NPs, 250 μg/mL CS or 50 μg/mL streptomycin (B-D) for 24 h. Biofilms incubated in TSB containing PBS were used as blank control. (A) *P. aeruginosa* (64 μg/mL CA NPs, 64 μg/mL CS or 13

μg/mL streptomycin); (B) *S. typhimurium*; (C) *L. monocytogenes*; (D) *S. aureus*. Biofilm cells were quantified by serial dilution plate counting method. Biofilm architectures after 24 h treatment were examined by scanning electron microscopy (E: *P. aeruginosa*; F: *S. aureus*). These experiments were performed three times with similar results each time. Error bars represent standard deviation. Scale bar represented 2 μm.

Fig. 4 CA NPs inhibit dispersed cells replication. Biofilm-dispersed cells were incubated for 24 h with 250 μg/mL CA NPs, 250 μg/mL CS or 50 μg/mL streptomycin. After then 10 μL samples was collected and incubated in 190 μL tryptone soya broth for 14 h. OD_{600} was detected. (A) *P. aeruginosa* and (B) *S. typhimurium*, (C) *L. monocytogenes* or (D) *S. aureus*.

Fig. 5 Growth curves of (A) *S. typhimurium* and (C) *S. aureus* obtained by culturing bacteria in TSB containing of CA NPs (250 μg/mL), CS (250 μg/mL) or streptomycin (50 μg/mL). CFU counting of (B) *S. typhimurium* (8 h) by 10^7-fold dilution and (D) *S. aureus* (8 h) by 10^5-fold dilution.

Fig. 6 CA NPs facilitated streptomycin accessibility into biofilms built by Gram-negative bacteria. (A) *P. aeruginosa* biofilms or (B) *L. monocytogenes* biofilms were exposed to CA NPs (125 μg/mL), CS (125 μg/mL) or streptomycin (25 μg/mL) for 1 h. Biofilms incubated with tryptone soya broth were used as blank control. Streptomycin residing in biofilms was examined by Immunofluorescence. Immunoreactivity was quantified by using Image Pro Plus. Scale bars = 10 μm.

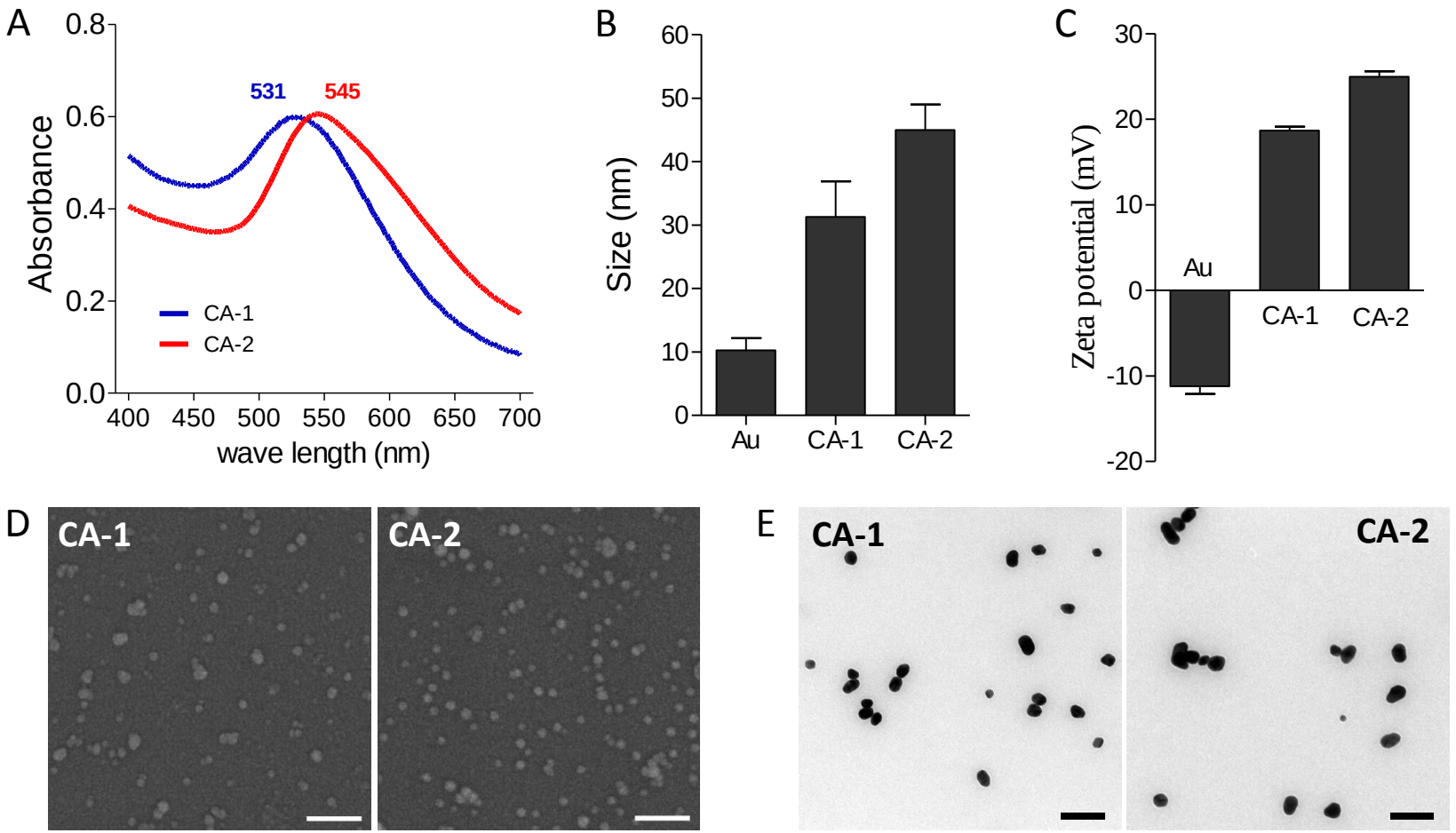

Fig. 1

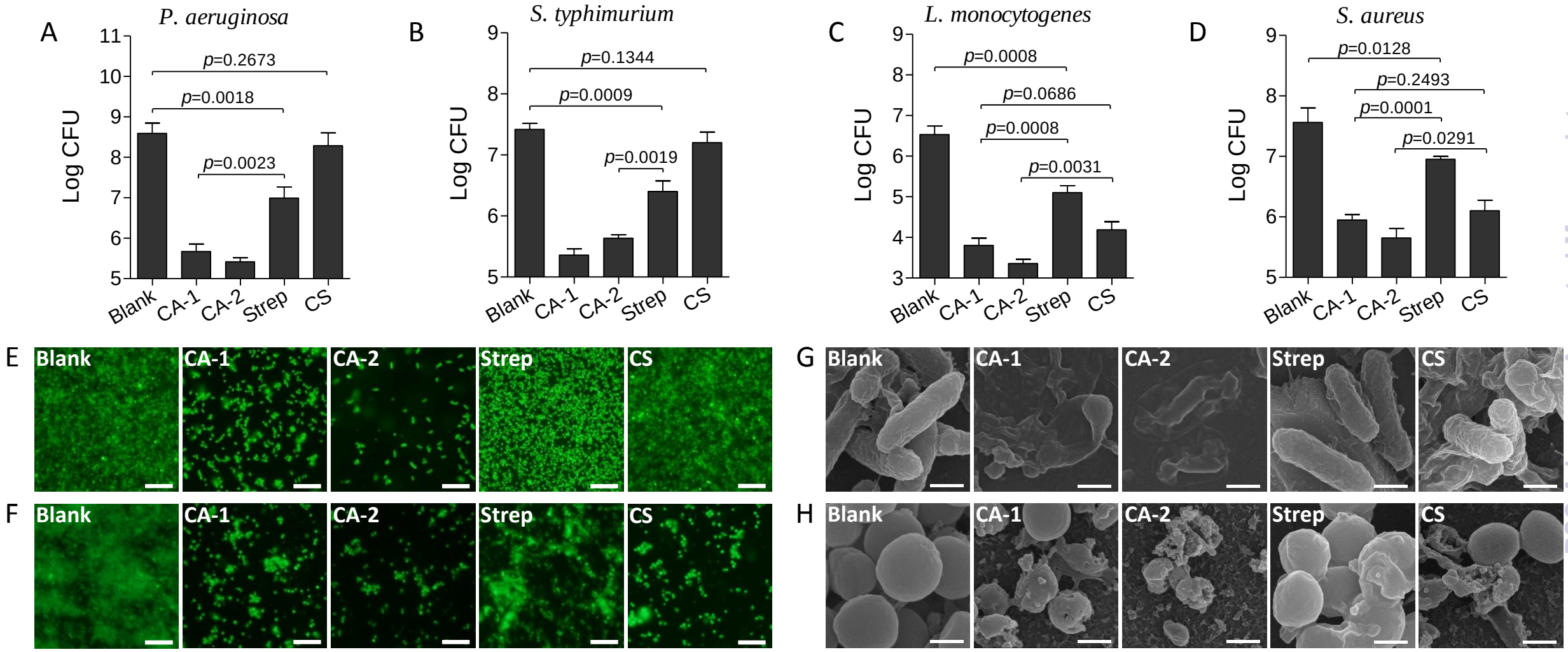

Fig. 2

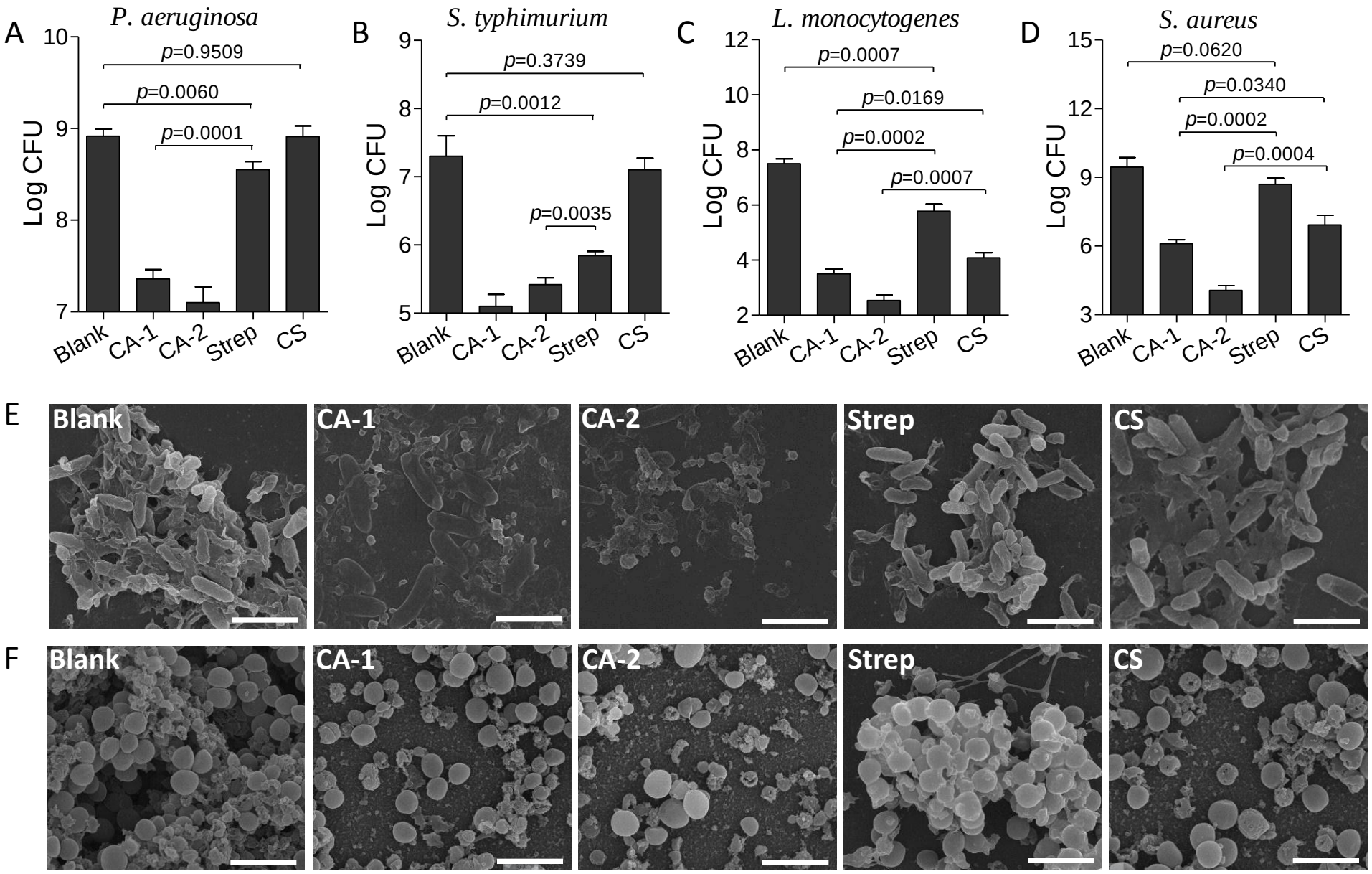

Fig. 3

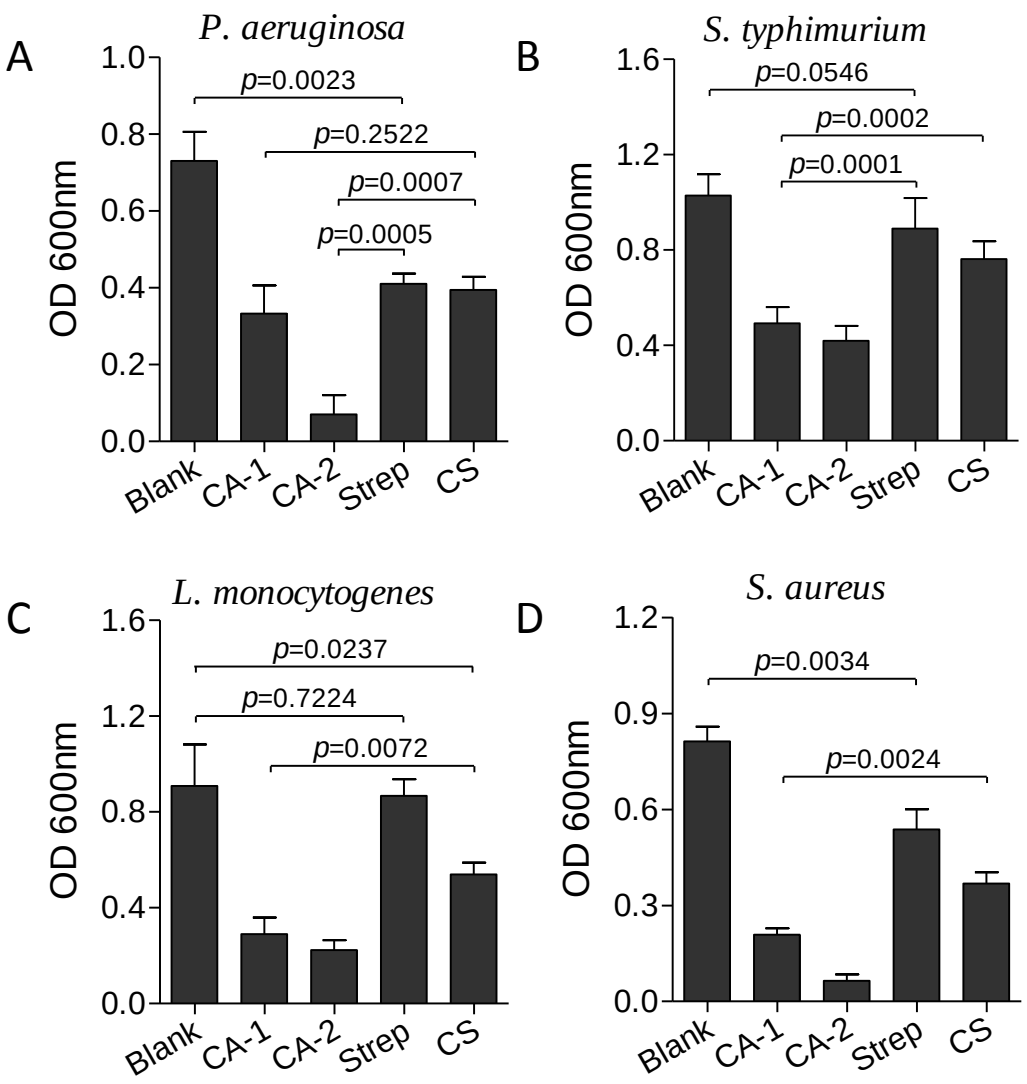

Fig. 4

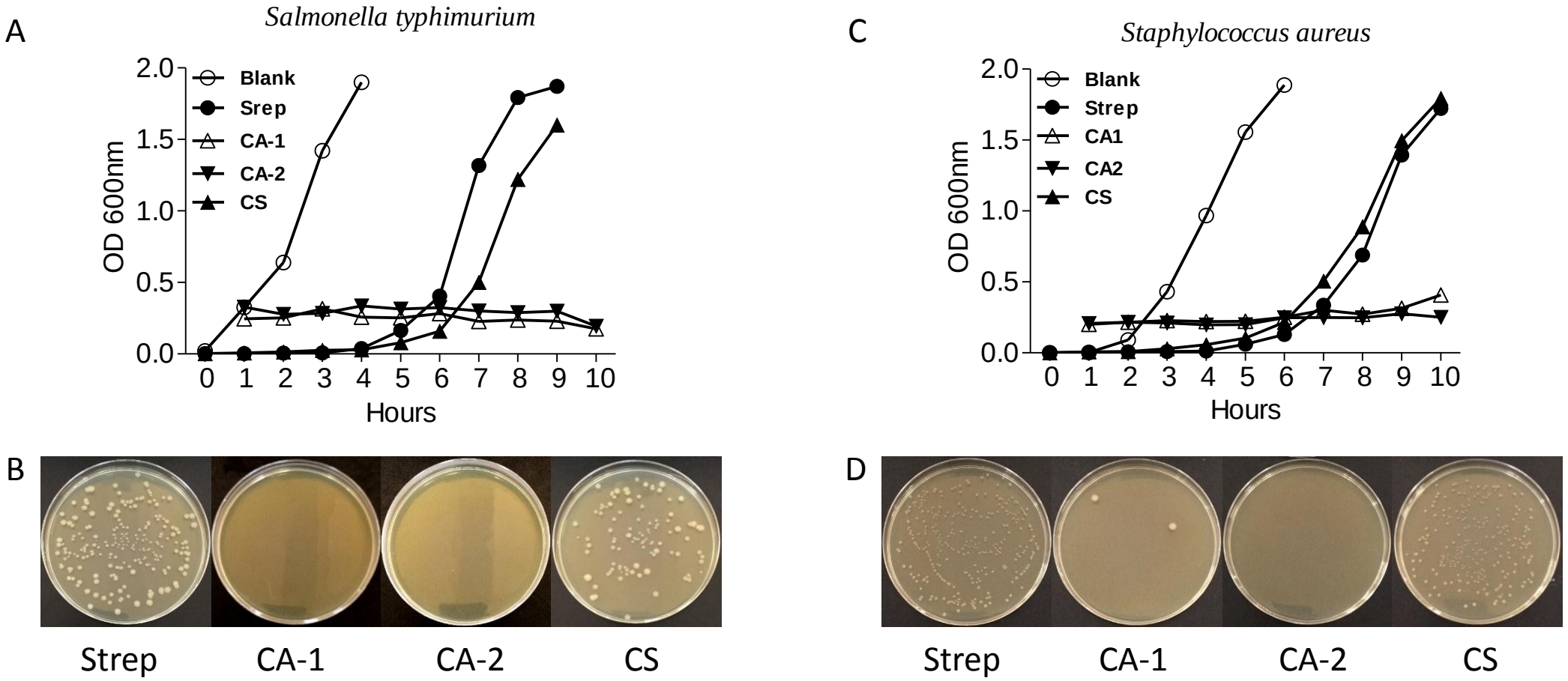

Fig. 5

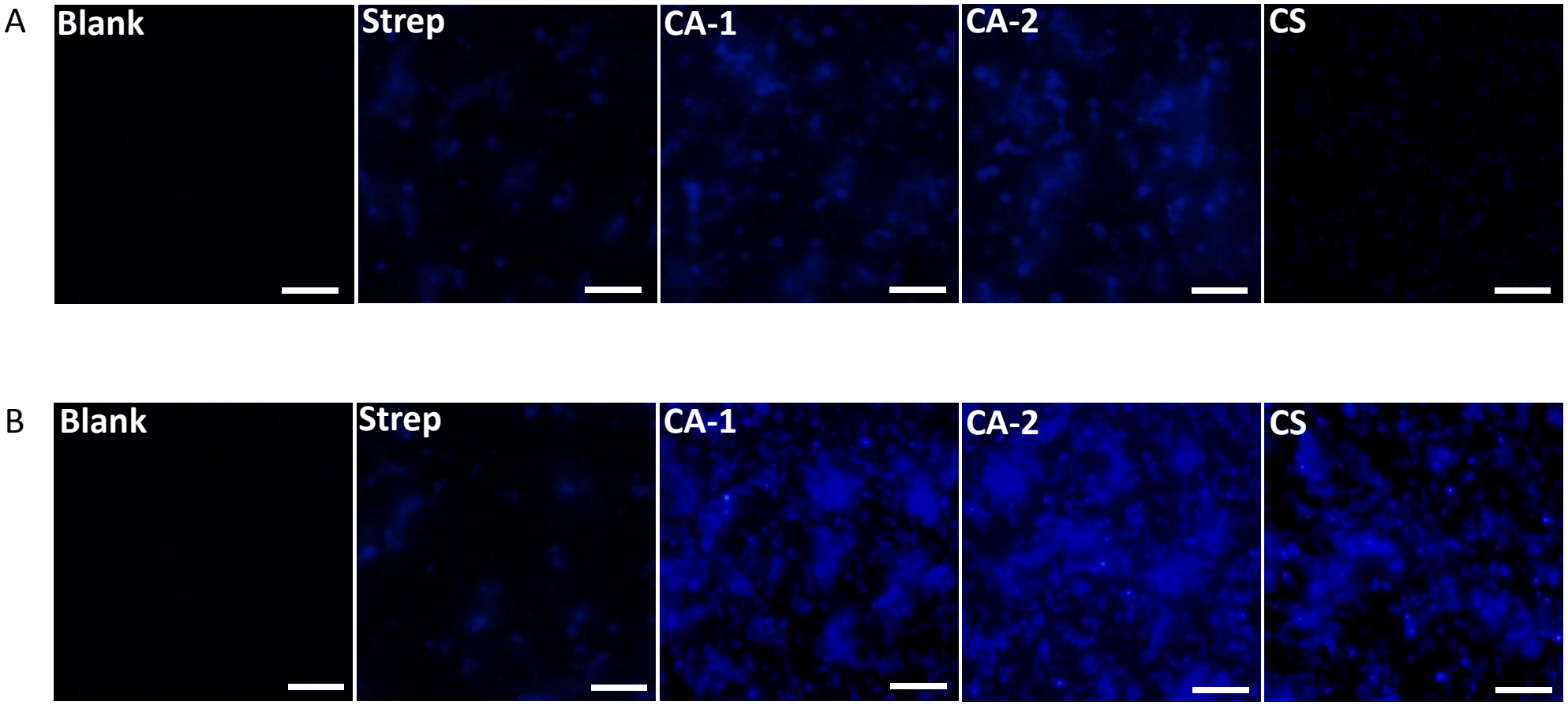

Fig. 6